

Panagiotopoulos, F., Shahgedanova, M. and Stephenson, D.B., 2002: 'A review of Northern Hemisphere winter-time teleconnection patterns', *European Research Course on Atmospheres (ERCA) – Vol. 5* (Ed. Claude Boutron), EDP Sciences, in press.

Abstract. This chapter reviews the major teleconnection patterns that occur in the boreal winter season. The history of teleconnection research is first reviewed emphasising the pioneering work of Sir Gilbert Walker. This is followed by a review of contemporary research that focuses on eleven teleconnection patterns classified into two groups: Euro-Atlantic and Pacific/North American patterns. Structure, impacts on weather and climate and temporal variability of each pattern are discussed by critically comparing major teleconnection studies. The lack of agreement on structure and occasionally the very existence of certain teleconnection patterns is also highlighted. These disagreements can be attributed to the absence of a universally accepted definition of teleconnections and the use of different statistical methods and data sets.

1. INTRODUCTION

The general circulation of the atmosphere exhibits significant variability on many different time scales. High frequency variations with periods less than 1-2 weeks are associated with transient eddies (synoptic systems) as seen on daily weather maps. Low frequency variations with periods longer than 1-2 weeks are related to coherent large-scale patterns of variation in the climate fields (e.g. pressure, temperature and precipitation).

The preferred modes of low-frequency atmospheric variability have been referred to as *teleconnections* (Ångström, [2]). There is no unique, universally accepted definition of teleconnections, but this term is used to describe the large-scale spatial dependencies in climate or more specifically spatial structures with two or more distinct and strongly coupled centres of action.

Teleconnections play an important role in the global climate system as they reflect coupling between the upper air quasi-stationary, planetary-scale circulation and short-term climatic fluctuations near the surface. They influence temperature and precipitation regimes and the location and intensity of the major jet streams and associated storm tracks. They are also responsible for anomalous weather patterns occurring simultaneously and persisting for a long period over different regions. In addition, teleconnections help to explain the transient behaviour of the stationary waves. Because of their importance, teleconnections often provide the scientific basis of operational long-range weather forecasts run by several national meteorological services around the world (e.g. the American NOAA/Climate Prediction Centre (CPC), <http://www.cpc.ncep.noaa.gov/data/teledoc/telecontents.html>). The complete knowledge of teleconnection patterns can be beneficial even to nowcasting or medium-range weather forecasting, as certain climate anomalies tend to occur simultaneously in conjunction with well-known teleconnection patterns. Weather forecasters can sometimes recognise poor guidance from Numerical Weather Prediction (NWP) models and amend their forecasts in such a way that the predicted evolution of weather systems is more consistent with teleconnection patterns.

This chapter aims to briefly describe the major teleconnection patterns in the extra-tropical regions of the Northern Hemisphere (NH) by summarising the most significant studies in the literature. The chapter begins with a brief historical review of teleconnection research and a more comprehensive review of the major recent studies followed by a detailed description of the individual primary teleconnection patterns. Finally, concluding remarks and general comments are presented in the last section.

2. REVIEW OF THE LITERATURE

Despite the popularity of the subject and the numerous advantages of having detailed knowledge of the behaviour and structure of teleconnection patterns, progress in teleconnection research has been relatively slow and unsatisfactory compared to other aspects of the meteorological science (e.g. weather forecasting). One of the main reasons is the lack of universally accepted criteria and procedures for defining teleconnection patterns. Different researchers have used different methods, data sets, meteorological variables, sampling periods and criteria resulting in a big variety of different, but often linearly dependent and overlapping patterns.

The earliest known use of the term `teleconnection` was by Ångström [2] who studied the well-known North Atlantic Oscillation (NAO, Walker and Bliss, [30]; van Loon and Rogers, [29]), although the concept itself had been recognised decades earlier. The primary goal of early teleconnection research was to establish relationships between the weather at different places of the world that could be used for seasonal forecasting (Walker and Bliss, [30]). The early approach was highly empirical and relied extensively on statistical techniques.

Sir Gilbert Walker pioneered early attempts to understand and identify low-frequency circulation modes. He was the first to use statistical regression to search for significant teleconnection patterns (though he did not actually use the term ‘teleconnections’). He introduced the use of correlation to study teleconnections and the use of multiple regression to the problem of long-range forecasting. His pioneering work culminated in the landmark paper of Walker and Bliss [30], which identified three dominant teleconnection patterns: the Southern Oscillation (SO), the North Atlantic Oscillation (NAO), and the North Pacific Oscillation (NPO).

The response to Walker’s work was initially positive as other researchers followed his example and adopted his approach to the investigation of empirical relationships in the atmosphere. Later, however, there was some criticism of his work, which may be responsible for the decline in the use of statistical approach in teleconnections research in the middle of the 20th century. The criticism focused on the degradation over time in strength of correlation-derived relationships and their physical interpretation. The increasing usage and improvement of physical and numerical methods in meteorological research and a general shift of interest towards short and medium-range weather forecasting also contributed to the decline of teleconnection research (see for example Stephenson *et al.* [25] for a complete historical review of NAO).

A renaissance was observed after 1960, mainly due to the great interest in the Southern Oscillation (SO) and its impacts on global climate. The usefulness of Walker’s empirical methods was widely recognised and many researchers applied them to the larger and higher quality data sets. Van Loon and Rogers [29] and Rogers [22] confirmed many of Walker’s results regarding the NAO and NPO. In their study of the seesaw in winter temperatures between Greenland and northern Europe, Van Loon and Rogers [29] constructed a new index for the NAO based solely on temperature differences between Greenland and Norway.

Wallace and Gutzler [32] were the first to provide a comprehensive and extensive summary of teleconnection patterns in the monthly averaged sea-level pressure (SLP) and upper-level geopotential height fields during the NH winter season. They used correlations and Principal Component Analysis (PCA), which they applied to a 15-year record of winter-time monthly averaged 500 hPa geopotential height fields. Wallace and Gutzler [32] constructed one-point correlation maps and introduced the concept of teleconnectivity, which helps to summarise one-point correlation maps of individual teleconnection patterns in just one map. They [32] defined teleconnectivity as the strongest negative

correlation on each one-point correlation map, plotted at the base grid point and they proposed it as a method of contrasting the strengths of teleconnection patterns for different base points. Figure 1 shows the teleconnectivity map for SLP and 500 hPa geopotential height. Figure 1a confirms the SLP patterns associated with the NAO and NPO as described by Walker and Bliss [30]. The dipole shaped pattern in the eastern North Pacific can be considered as a reflection of another major teleconnection, the Pacific/North American pattern (PNA).

The mid-tropospheric teleconnectivity map (Fig. 1b) shows a more complex picture: teleconnection patterns tend to be stronger but of regional nature. Wallace and Gutzler [32] identified five major patterns at the 500 hPa level, which they named on the basis of their geographical location. These are: the Western Pacific (WP), Western Atlantic (WA), Eastern Atlantic (EA), Pacific/North American (PNA) and the Eurasian patterns. The first two are dipole shaped patterns over the western sectors of the oceans, whereas PNA is a quadruple shaped pattern in the eastern North Pacific-North America area.

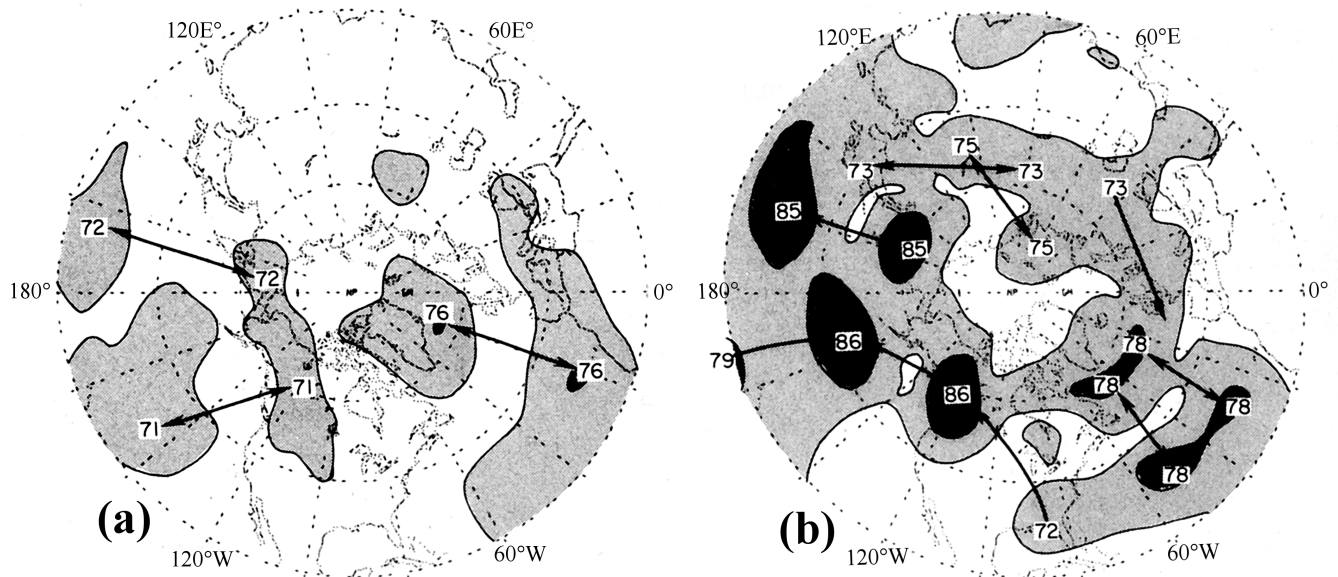


Figure 1. Strongest negative correlation (ρ_i) on each one-point correlation map, plotted at the base grid point (referred to in the text as ‘teleconnectivity’) for (a) SLP and (b) 500 hPa geopotential height. Negative signs have been omitted and correlation coefficients multiplied by 100. Regions where $\rho_i < 60$ are unshaded; $60 \leq \rho_i \leq 75$ stippled lightly; $75 \leq \rho_i$ stippled heavily. Arrows connect centres of strongest teleconnectivity with the grid point, which exhibits strongest negative correlation on their respective one-point correlation maps (from Wallace and Gutzler [32]).

The EA pattern has two centres in the eastern North Atlantic and a third one near the Black Sea whereas the Eurasian pattern corresponds to a large-scale wave train stretching eastward from Scandinavia to Japan across Eurasia (Fig. 1b). Wallace and Gutzler [32] attempted to reproduce these teleconnection patterns using an independent data set. All the patterns were reproduced (with PNA reproduced best), but most patterns were expressed worse than in the original data set. In addition, the leading eigenvectors of the correlation matrix of the monthly mean 500 hPa geopotential height field contained elements of the regional patterns revealed in the one point correlation maps.

Horel [9] confirmed many of the teleconnection patterns identified by Wallace and Gutzler [32] by using the rotated PCA (RPCA), which explains maximum total variance with minimum spatial patterns (Ambaum *et al.* [1]). The reader is referred to Richman [21] for an extensive review of this method and to Barnston and Livezey [4] for a comparison between this method and the spatial correlation method used by Wallace and Gutzler [32].

Another major study of the low-frequency variability in the atmospheric circulation was conducted by Esbensen [7]. By using a 30-year record of monthly averaged 700 hPa geopotential height and the

method of spatial correlation analysis, he distinguished between the interannual and intraseasonal variability. In the intraseasonal band, Esbensen [7] confirmed three of the five patterns identified by Wallace and Gutzler [32] (namely WA, WP and PNA) and found a new pattern over Asia (which was discussed by Wallace and Gutzler [32] but not identified as a distinct teleconnection pattern). These patterns are summarised in the teleconnectivity map shown in Fig. 2a. The two dipole shaped patterns observed in the western sectors of the North Atlantic and North Pacific Oceans are WA and WP respectively, whereas PNA has three centres in North Pacific, south-western Canada and the south-eastern United States.

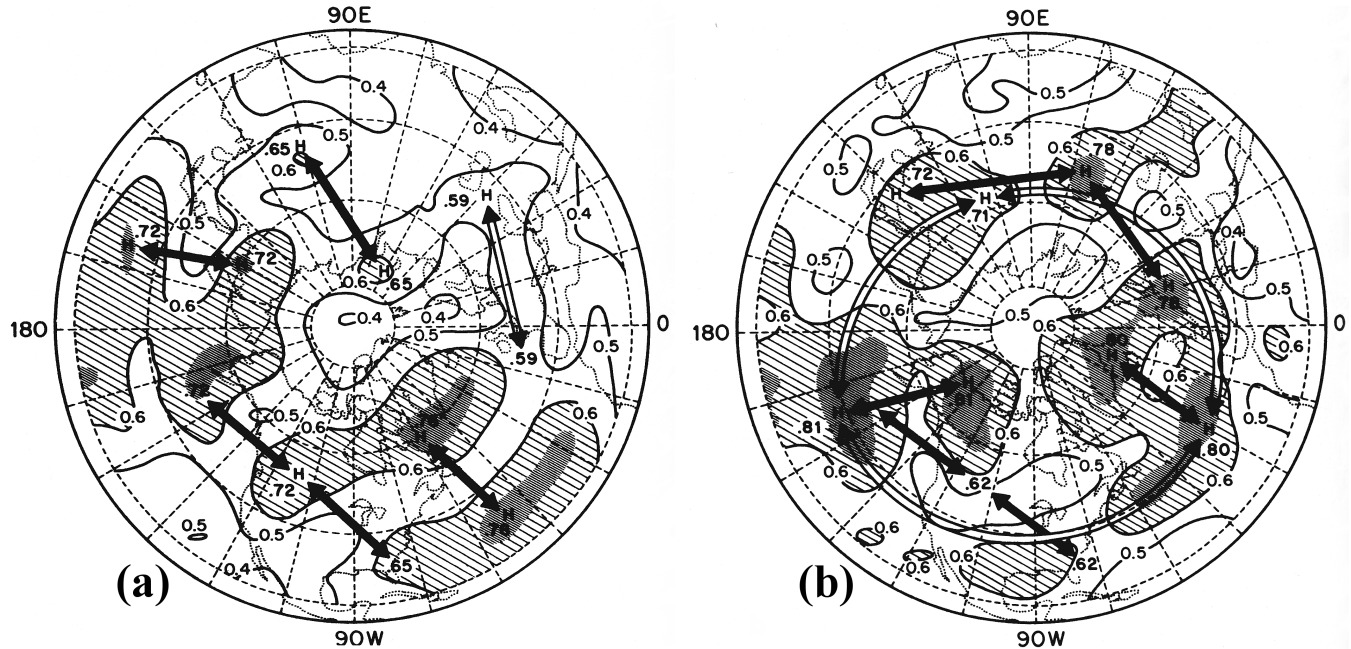


Figure 2. Teleconnectivity (ρ_i) field of (a) the intermonthly signal and (b) the interannual signal. Regions where $\rho_i < 0.6$ are unshaded; $0.6 \leq \rho_i \leq 0.7$ lightly shaded and $0.7 \leq \rho_i$ dark shaded. Contour interval is 0.1. Dark arrows indicate teleconnection patterns that are supported by both the teleconnectivity and the one-point correlation maps; the light arrows are based on the one-point correlation maps only (from Esbensen [7]).

Inspection of the interannual teleconnectivity map (Fig. 2b) reveals a different and more complex picture. Only PNA is reproduced whereas the rest of the patterns from the intermonthly band are missing. The Eurasian pattern, which was absent in the intermonthly band, is prominent in the interannual one. Another pattern identified by Esbensen [7] is a dipole-shaped pattern with centres in the North Pacific and north-western Canada, which he referred to as the North Pacific pattern (NP) due to its similarity to the pattern first identified by Walker and Bliss [30]. Another pattern with centres in the North Atlantic, North Pacific and over Lake Baikal is named by Esbensen ‘zonally symmetric seesaw’ because of its similarity to the SLP pattern described by van Loon and Rogers [29]. Esbensen [7] briefly discussed correlations between the teleconnection patterns. Most teleconnection patterns were independent but NP, zonally symmetric seesaw and PNA were weakly correlated in the interannual band. Esbensen [7] noted, however, that this interpattern correlation might be influenced by the fact that all three patterns share a common centre in the north-eastern Pacific Ocean.

A comprehensive study of teleconnection patterns was performed by Barnston and Livezey [4]. They used RPCA to analyse a 34-year record of 700 hPa geopotential height data. Their analysis was designed to emphasise interannual variability but because a short, 1 month averaging interval was used, it also contained some elements of intraseasonal variability. Barnston and Livezey [4] identified nine major teleconnection patterns with NAO and PNA being the dominant modes of variability for the winter months. Patterns analogous to those of Wallace and Gutzler [32] were also found, such as WP and EA,

and two new patterns over the Pacific, which were named the Eastern Pacific (EP) and North Pacific (NP) patterns. In addition, Barnston and Livezey [4] found three distinct patterns over Eurasia and a new pattern extending over North America, which they referred to as the Tropical/Northern Hemisphere pattern (TNH).

Barnston and Livezey [4] attempted to reproduce their patterns using 10-day mean 700 hPa geopotential height data. Most patterns were found but accounted for a smaller portion of the total variance. They also attempted to exploit predictive potential of teleconnection patterns by considering autocorrelation of the principal components (PCs), but no significant autocorrelations have been found. The WP pattern was the only one to show a significant amount of persistence but in general, correlations were rather weak. Barnston and Livezey [4] pointed out that further research is needed in order to verify the predictive potential of the teleconnection patterns.

Blackmon *et al.* [6] constructed one-point correlation maps using an 18-winter data set of 500 hPa geopotential height. Three averaging periods were used: long (30-90 days), intermediate (10-30 days) and short (2.5-6 days). The one-point correlation maps for the 30-90 day period (not shown) resembled the teleconnection patterns described by Wallace and Gutzler [32]. Blackmon *et al.* [6] confirmed Wallace and Gutzler's result [32] that these patterns resembled discrete standing oscillations with geographically fixed centres. In contrast, the intermediate variability was dominated by zonal wave trains, which didn't have preferred geographical positions and were confined within continental waveguides. The centres of action of these patterns were elongated in the meridional direction and they did not exhibit a preferred longitudinal phase. These results were confirmed by Schubert [23] who found that the leading eigenvector patterns of the band-pass filtered 500 hPa geopotential height field changed from meridionally elongated wave trains to zonally elongated dipoles as the period of fluctuations increased.

Kushnir and Wallace [14] confirmed the results obtained by Blackmon *et al.* [6] by using RPCA applied to a 39-year data set of 500 hPa geopotential height. Kushnir and Wallace [14] distinguished between intermediate (10-60 days), intermonthly (60-180 days) and interannual (longer than 180 days) variability. They found that zonally oriented wave trains dominate the intermediate variability band over the continents, but meridionally oriented dipole shaped patterns prevail at lower frequencies over the oceans. PNA and NAO were the best defined patterns in the interannual variability while WA stands out clearly in the intermonthly variability band.

There have been relatively few recent studies focussing on low frequency atmospheric variability. Pavan *et al.* [20] applied PCA to the winter-time (December-March) monthly averaged 500 hPa geopotential height anomalies using the high resolution NCEP/NCAR re-analysis data set. NAO, PNA, EA, the Scandinavian pattern and WP were amongst the patterns confirmed. The relation between many teleconnection patterns and local weather ("blocked" and "zonal") regimes was also emphasised in their study. Pavan *et al.* [19] found that the EA and the Scandinavian patterns are associated with the occurrence of El-Nino-like sea surface temperature (SST) anomalies. They also suggested that the effects of NAO forcing by extra-tropical SSTs are more evident on interdecadal than intradecadal variations.

Figure 3 provides a more up-to-date and easily accessible summary of the major teleconnection patterns obtained by RPCA of monthly mean 700 hPa geopotential height anomalies for 1964-1994 (the data was kindly provided by Dr Gerry Bell from the Climate Prediction Centre (CPC), at the National Centres for Environmental Prediction (NCEP) of the American National Oceanic and Atmospheric Administration (NOAA)). The maps correspond to the positive phase of each pattern during the month of January.

3. EURO-ATLANTIC TELECONNECTION PATTERNS

A more detailed description of the major winter-time teleconnection patterns in the North Atlantic/European area is presented in this section. Emphasis is given on the NAO due to its dominant nature, its major impact on European weather and climate and its extensive documentation in the literature.

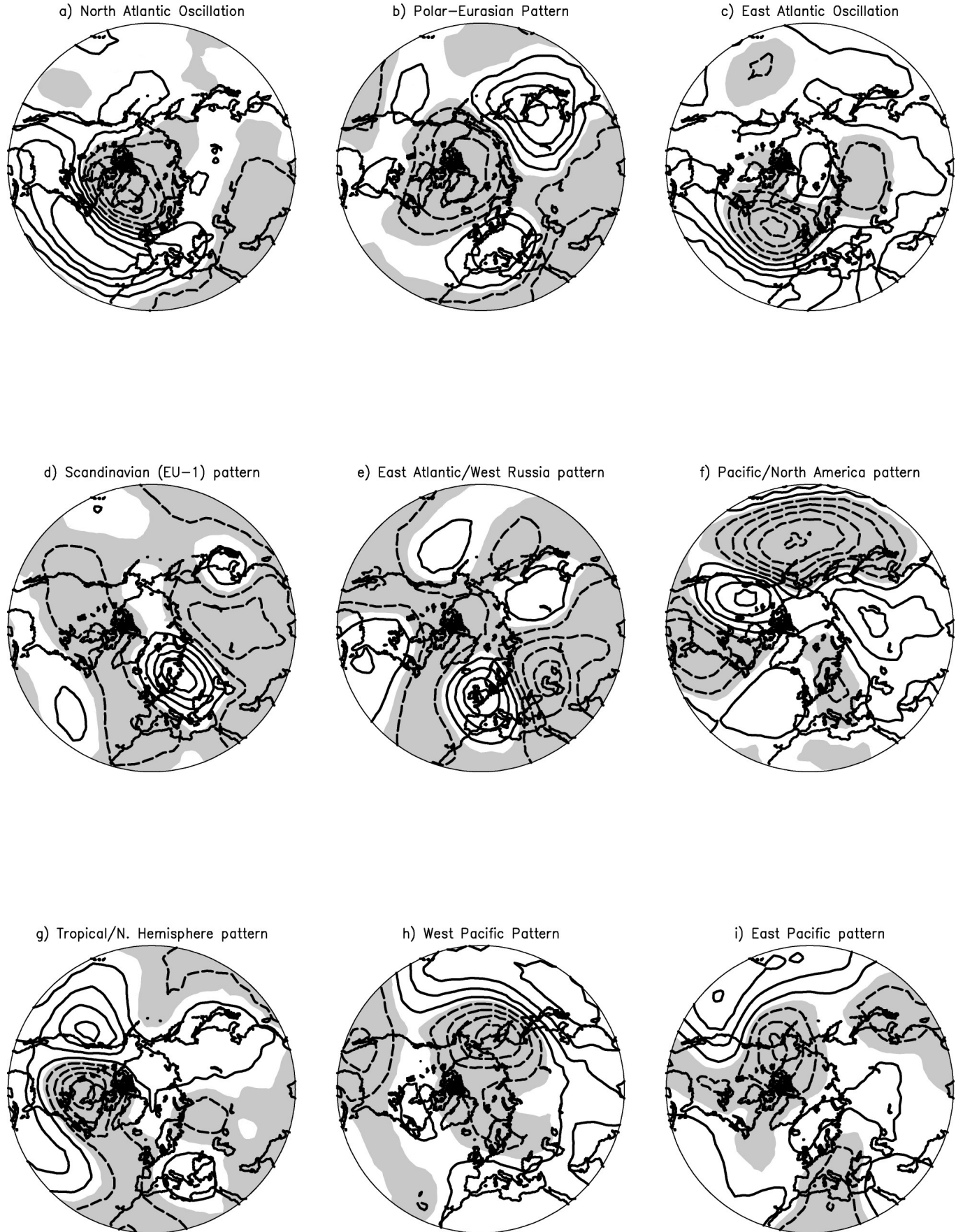


Figure 3. Northern Hemisphere teleconnection patterns for January based on a rotated principal component analysis (RPCA) of monthly mean 700 hPa geopotential height (kindly provided by the CPC). Grey shading indicates negative loading weights and contours are marked for loading weights of 0.1, 0.3, 0.5, 0.7 and 0.9 (solid) and -0.1, -0.3, -0.5, -0.7 and -0.9 (dashed). The panels show the following patterns: a) NAO, b) Polar Eurasian, c) Eastern Atlantic, d) Scandinavian (EU-1), e) Eastern Atlantic/Western Russian, f) PNA, g) Tropical/Northern Hemisphere, h) Western Pacific and i) Eastern Pacific.

3.1 North Atlantic Oscillation (NAO)

The North Atlantic Oscillation (NAO) is one of the most prominent teleconnection patterns (Fig. 3a). It is a dipole pattern associated with a large-scale net displacement of air between the two negatively correlated centres over Greenland and subtropical North Atlantic. Walker and Bliss [30] constructed an index consisting of a linear combination of surface air temperature (SAT) and SLP data from selected stations. The pressure, temperature and precipitation correlation patterns are illustrated in Figure 4.

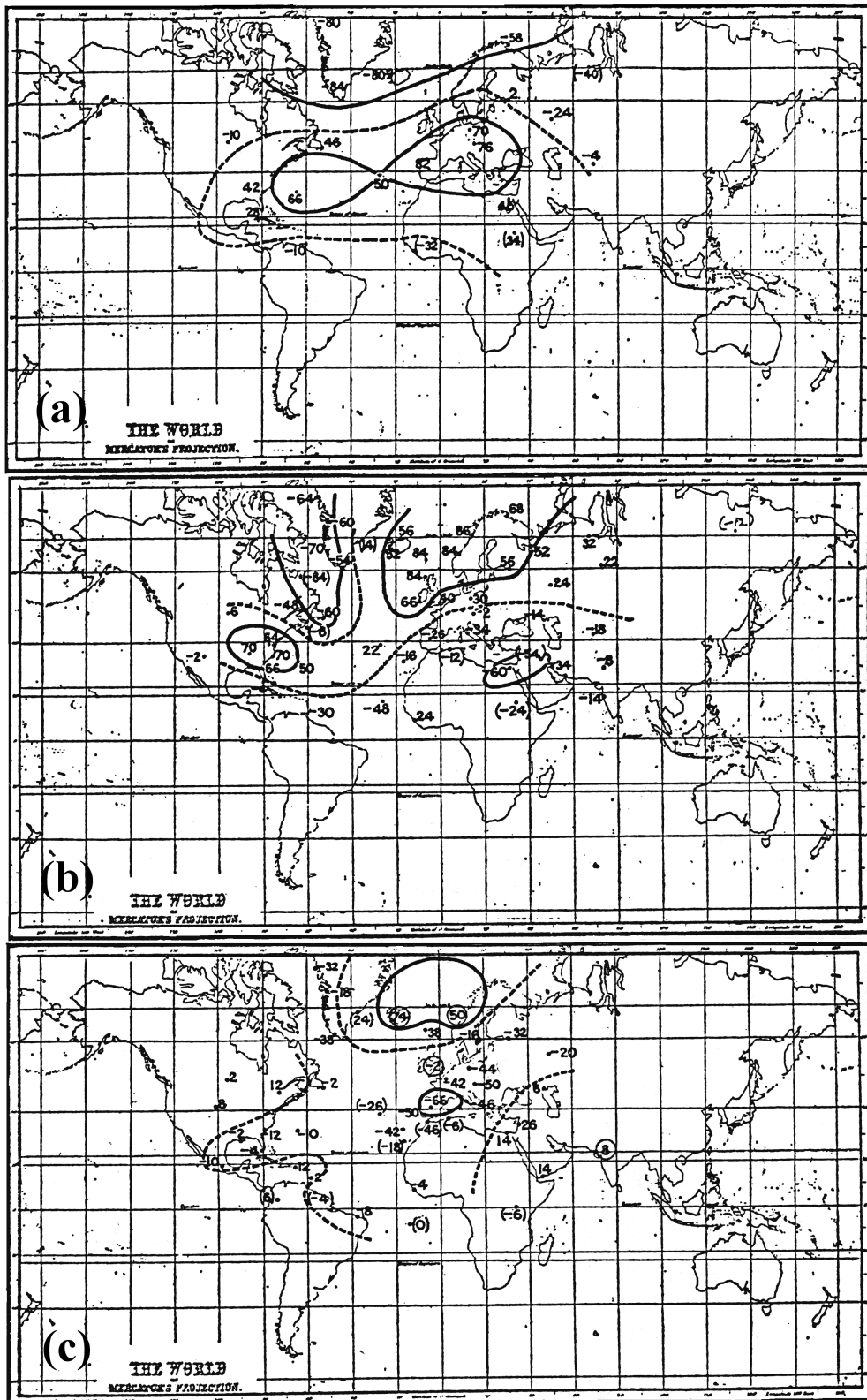


Figure 4. Correlation coefficients of (a) pressure, (b) temperature and (c) precipitation data for selected stations with the NAO index for winter (December – February (DJF), from Walker and Bliss, [30]).

The positive phase of the NAO is characterised by a deeper than normal Icelandic low, a more intense subtropical anticyclone in the southern North Atlantic (the Azores high) and an enhanced westerly flow across the North Atlantic and north-western Europe (Fig. 3a and 4a). During the negative phase, the centres of action are weaker than usual. Both positive and negative phases of the NAO force temperature anomalies in Europe and North America (Fig. 4b). More importantly, high winter temperatures are observed in northern Europe and eastern US during the positive phase of the NAO.

Walker and Bliss [30] pointed out that the relationship between the NAO and weather is consistent with simple dynamical arguments: a deeper than normal Icelandic low is accompanied by a more northerly flow and cold advection over the Greenland-Labrador area and an enhanced south-westerly flow of mild, maritime air over north-western Europe. A predominantly south-westerly flow normally prevails over the eastern United States and cool, north-westerly flow over the Middle East with a southward displaced storm track in that region. Precipitation is enhanced in the north-eastern Atlantic, Scandinavia and the Middle East and reduced over southern Europe and the Mediterranean Sea (Fig. 4c).

Van Loon and Rogers [29] investigated the relationship between the NAO and temperature using a 46-year winter temperature data set, which was unavailable to Walker and Bliss [30], focusing on the temperature see-saw between Greenland and northern Europe. Their study revealed another important aspect of the NAO which had not been previously noted: high NAO winters with lower than normal temperatures in the Greenland-Labrador region (their Greenland above (GA) state) were found to be characterised not only by a deeper than normal Icelandic low, but also by a weaker than normal Aleutian low with positive SLP anomalies in the middle latitudes of the central North Pacific.

The NAO was also identified by Wallace and Gutzler [32] in their SLP teleconnectivity field (Fig. 1a). Their one-point correlation map (Fig. 5) is similar to the plot of Walker and Bliss (Fig. 4a). One important difference is the absence of the north-eastward shift of the low-latitude centre of action towards southern Europe and the Mediterranean Sea.

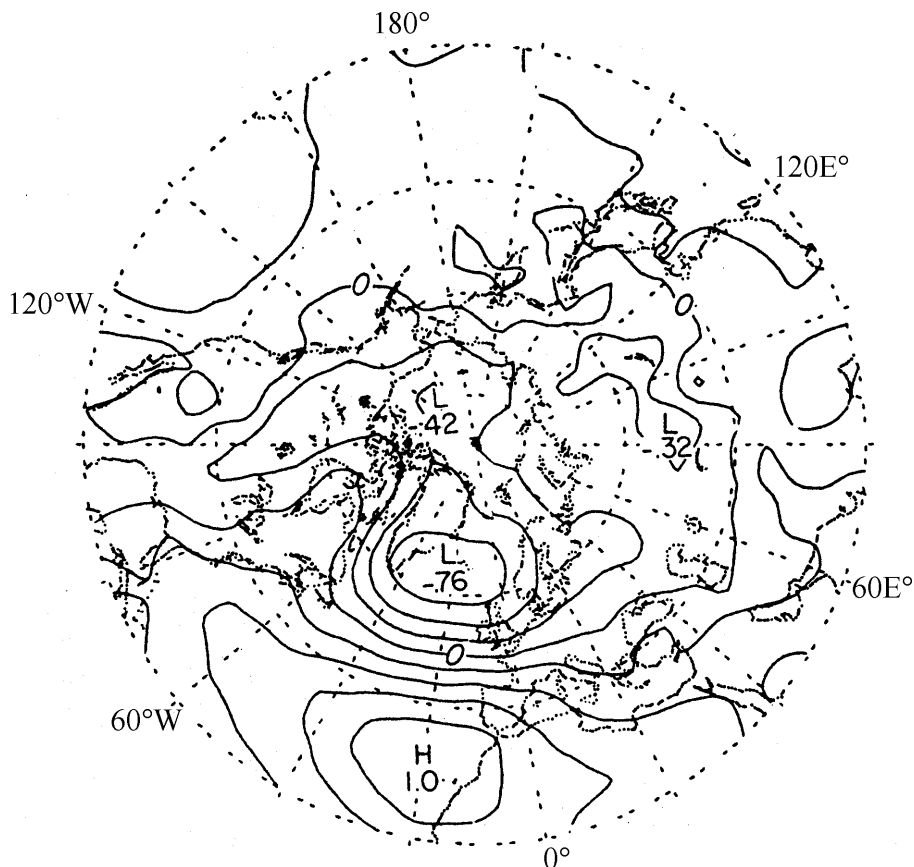


Figure 5. One-point correlation map showing correlation coefficients between SLP at the grid point 30°N, 20°W, and SLP at every grid point. Contour interval is 0.2 (from Wallace and Gutzler, [32]).

The existence and characteristics of the NAO were confirmed in many other studies. Barnston and Livezey [4] for example, ranked the NAO as the strongest contributor to low-frequency variability in the geopotential height fields in the NH. Figure 6 shows the NAO as identified in their RPCA. Again, there are two strong major centres in the North Atlantic, which are displaced about 5° to the east of the corresponding map by Wallace and Gutzler (Fig. 5). Evident is also the north-eastward shift of the low-latitude centre towards southern Europe. There are also two secondary centres negatively correlated with the Greenland centre. The first one is over central United States and the second and weaker centre can be seen over the eastern coast of Asia.

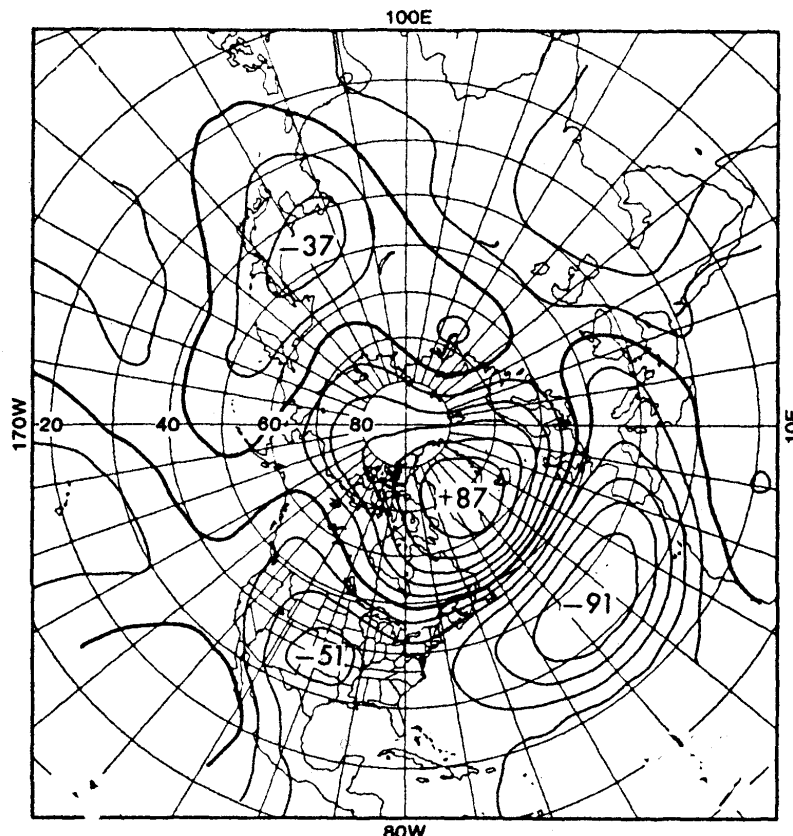


Figure 6. The North Atlantic Oscillation (NAO) in January as depicted in the RPCA of Barnston and Livezey [4].

Many different indices of the NAO have been defined by various researchers. Table 1 shows the most widely used NAO indices (NAOIs).

Table 1. Details of different NAO indices

Researcher(s)	Meteorological Variable	Period
Walker and Bliss [30]	Linear combination of SLP and SAT in selected stations	1875-1930
Hurrell [12]	Difference of normalised SLP between Lisbon (Portugal) and Stykkisholmur (Iceland)	1864-1994
Van Loon and Rogers [29]	Difference in SAT between Jakobshavn (Greenland) and Oslo (Norway)	1860-1975
Stephenson <i>et al.</i> [24]	DJF mean surface temperatures averaged over large regions covering NW Europe and NW Atlantic	1900-1994
Jones <i>et al.</i> [13]	Difference between normalised pressure in Gibraltar and Reykjavik	1823-1996

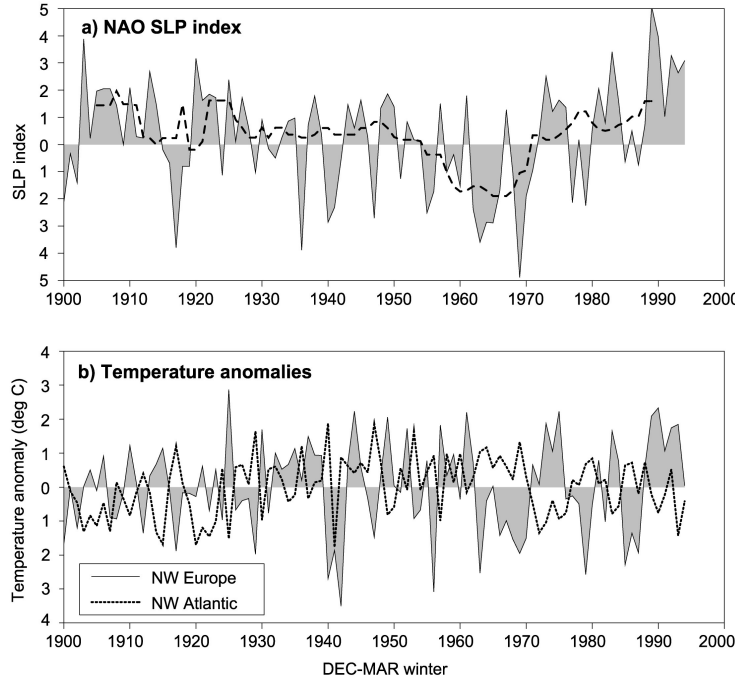


Figure 7. Time series of (a) the NAO SLP index: difference in standardised December – March mean SLPs between Lisbon (Portugal) and Stykkisholmur (Iceland). The 10-year running median is shown by the dashed line; (b) DJF mean surface temperature averaged over large regions covering NW Europe (from Stephenson *et al.* [24]).

Inspection of these indices (Fig. 7a) suggests that the NAO exhibits substantial interannual and interdecadal variability. The NAOI was positive from the turn of the century until about 1930 with strong westerly flow and higher than normal temperatures over the North Atlantic and north-western Europe. From the early 1940s until the early 1970s the NAOI exhibited a downward trend with weak westerlies over the Atlantic and lower than normal temperatures over most of Europe (Fig. 7b). During the last 30 years, a sharp reversal has occurred with highly positive NAOI values.

Hurrell [12] suggested that decadal variability in the NAO has become much more pronounced since 1950. By comparing temperature departures with decadal trends in the NAO, he concluded that positive temperature anomalies over Europe during 1985–1995 were strongly related to the persistent and exceptionally strong positive phase of the NAO. He also found that during periods of high NAOI, the axis of maximum moisture transport acquires stronger submeridional (south-west to north-east) orientation across the North Atlantic and northern Europe. Hurrell [12] linked this shift and precipitation anomalies over Europe. A significant reduction in the atmospheric moisture transport and reduced precipitation occur in southern Europe and the Mediterranean, while precipitation is enhanced in north-western Europe.

There are numerous studies on the impacts of NAO on weather and climate and the response of terrestrial and oceanic ecosystems. A comprehensive review of many of those studies together with more extensive information about the NAO can be found in the recent American Geophysical Union (AGU) Monograph [25].

In recent years, the identity of the NAO has become a subject of a debate (Wanner *et al.* [33]). An alternative teleconnection, termed the Arctic Oscillation (AO, also known as Northern Annular mode (NAM)), has been proposed by Thomson and Wallace [27, 28], who argued that the AO shows a closer link with Eurasian SAT than the NAO. They found that the AO resembles the NAO but its primary centre covers more of the Arctic. The AO exhibits a distinct signature in the geopotential height and temperature fields marked by a zonally symmetric, equivalent barotropic structure. Thompson and Wallace [26] also linked the recent climatic trends (warming of the lower troposphere over Eurasia) with the AO and the strengthening of the westerlies at subpolar latitudes with weakening of the jet stream at low latitudes. There is a strong difference in opinions among the meteorological community on which teleconnection pattern, NAO or AO, is dominant and more appropriate to use. Ambaum *et al.* [1] concluded that NAO is more physically relevant and robust for NH variability than AO, whereas Wallace [31] suggested that NAO and AO are two paradigms of the same phenomenon. He argued that these cannot be equally valid and he proposed some methods of distinguishing between them.

3.2 Polar/Eurasian pattern

The Polar/Eurasian (PE) pattern is a prominent mode of winter-time low-frequency variability in the Northern Hemisphere. It consists of one main centre of geopotential height anomalies over the Arctic and two broad oppositely signed centres over Europe and Eastern Siberia and the Far East (Fig. 3b). The positive phase of the pattern is associated with a deeper than normal polar vortex and higher than normal geopotential height values over the entire Eurasia. The negative phase is associated with anomalies in the opposite sense.

Esbensen [7] found a similar pattern in both the intermonthly and the interannual periods of his study Thompson and Wallace's [26] definition of the AO as the leading EOF of the winter-time SLP field has a similar structure to the Polar/Eurasian pattern. They pointed out that the AO can be interpreted as the surface signature of modulations in the strength of the upper level polar vortex. The time series of the pattern exhibits substantial interannual and interdecadal variability (not shown). The negative phase is characterised by colder than average winters over most of Eurasia and it dominated between 1964/65 and 1969/70 and again from 1976 to 1986. Persistent positive phases of the pattern are observed from 1971-1976 and in the last decade, both characterised by a succession of mild winters.

3.3 Eastern Atlantic (EA) pattern

The Eastern Atlantic pattern (EA) was first identified by Wallace and Gutzler [32]. The EA pattern is characterized by two same-sign centres located south-west of the Canary Islands (25°N , 25°W) and between the Black and Caspian Seas (45°N , 40°E) and two centres of opposite sign located west of the British Isles and over central Siberia (60°N , 100°E , Fig. 3c and 8).

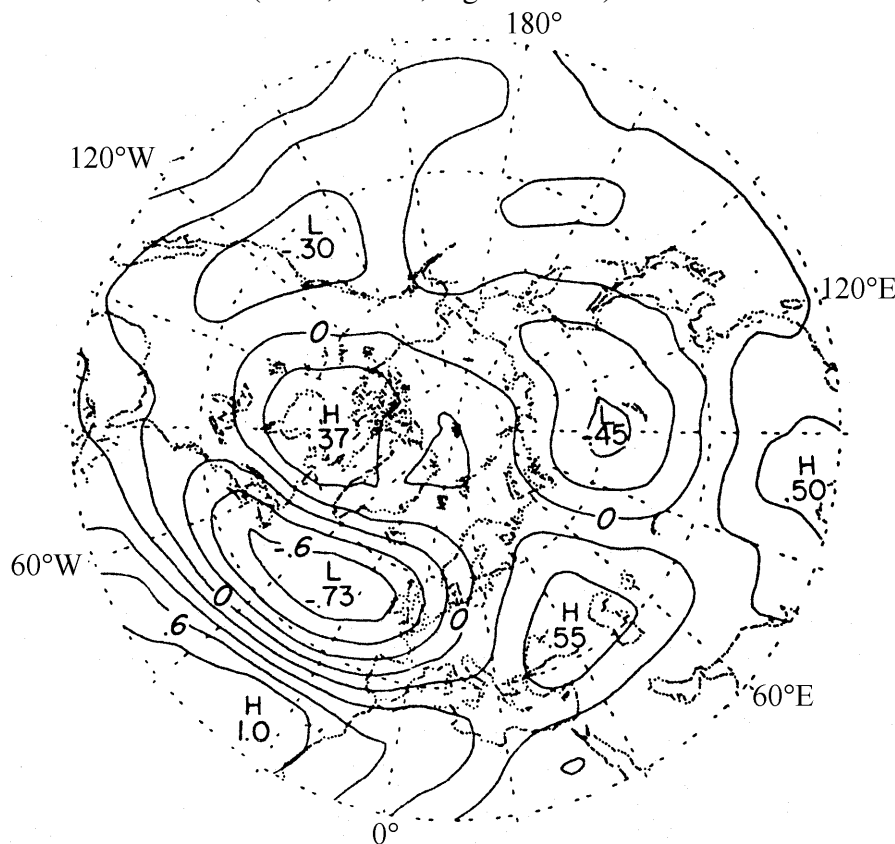


Figure 8. One-point correlation map showing correlation coefficients between SLP at the grid point 25°N , 25°W and SLP at every grid point (from Wallace and Gutzler, [32]).

Wallace and Gutzler [32] defined an index of EA (EAI) based on normalised 500 hPa geopotential height anomalies at the centres (not shown). Positive values of the EAI are associated with the presence of a strong ridge off the West European coast and a trough extending from the Barents Sea towards the

Mediterranean Sea. Analysis of the composite maps of 1000-500 hPa thickness has shown that this pattern exhibits an equivalent barotropic structure.

The EA pattern was also identified by Horel [9] and by Esbensen [7] in the intermonthly band. In the latter analysis, the northern centre was displaced eastwards in comparison with the pattern obtained by Wallace and Gutzler [32]. Barnston and Livezey [4] and Kushnir and Wallace [14] found another version of the EA pattern, characterised by a dipole shaped structure and the absence of a well defined third centre (Fig. 9a and 9b respectively). The EA is often confused with the NAO because of their structural similarities but comparison of Fig. 9a with Fig. 6 of the NAO shows that the NAO has only two centres in the North Atlantic without any centre over Eurasia.

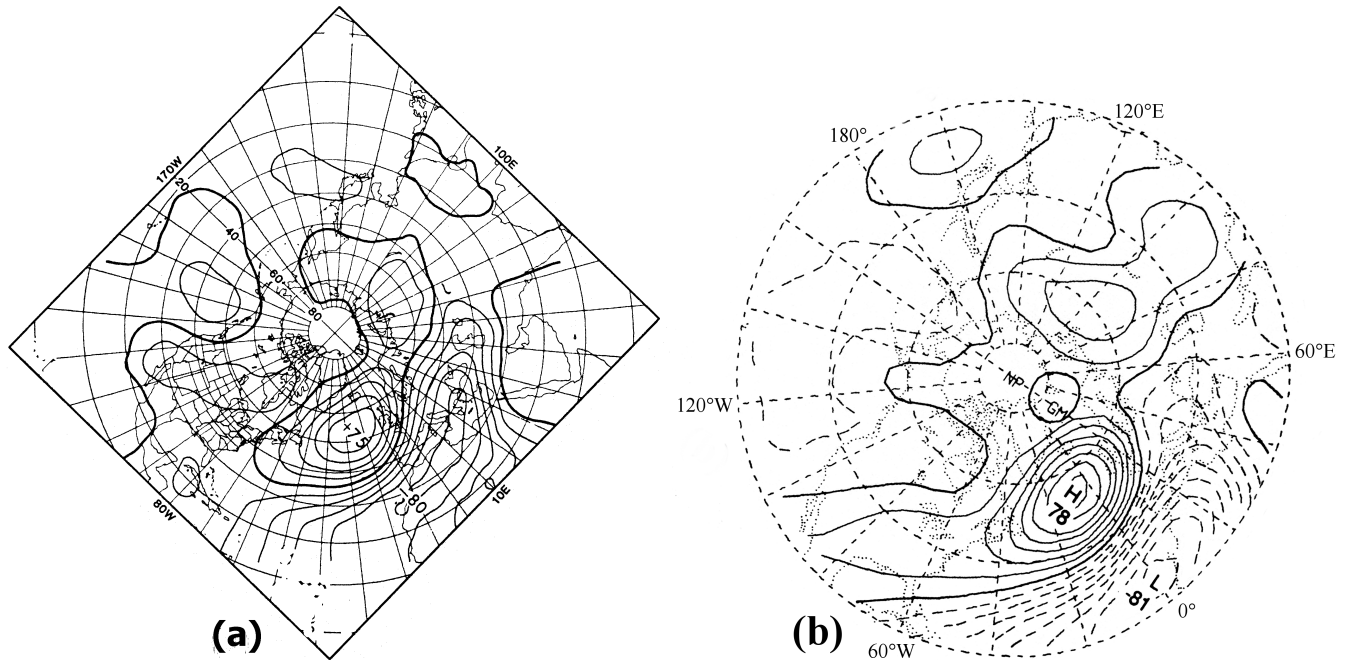


Figure 9. (a) The Eastern Atlantic (EA) pattern in February January as depicted in the RPCA of Barnston and Livezey [4]; (b) Loading vectors of the leading principal components of the intermonthly (60 – 180 day period) variability over the North Atlantic. Contour interval 0.1; negative contours are dashed. Decimal points are omitted on labels for extrema (from Kushnir and Wallace, [14]).

3.4 Scandinavian (EU-1) pattern

The Scandinavian pattern is a robust pattern of low-frequency circulation over the North Atlantic and Eurasia. It is identified in many teleconnections studies but often with large differences. Barnston and Livezey [4] showed that the Scandinavian pattern (they referred to it as the Eurasian Type 1 pattern) has three centres (Fig. 3d and 10): over Finland/north-western Russia (60°N , 40°E); over western Mongolia (50°N , 180°E); and over south-western Europe (45°N , 0°E). Two weaker centres are found over Japan and central North Atlantic (35°N , 90°E , Fig. 10). The positive phase of the Scandinavian pattern is associated with the presence of a blocking anticyclone over north-western Russia or eastern Scandinavia, upper level troughs over Western Europe and Central Asia and a ridge over the Far East.

Esbensen [7] found the Scandinavian pattern in both the intermonthly and interannual bands. However, in his analysis, the pattern had a different structure: a ridge over the Far East was present but there was no upper level trough over Western Europe. Wallace and Gutzler [32] found a similar pattern, which they referred to it as the Eurasian pattern, characterised by a westward shift of the centres, a well-defined centre over the Far East and the absence of the Western European centre. The time series of the Scandinavian pattern index (not shown) exhibits large intraseasonal, interannual and interdecadal variability. Negative phases of the pattern, characterised by lower than average pressure in north-eastern Europe and the extension of the Azores high in Western Europe were observed from 1964-1980 and again from 1986-1993.

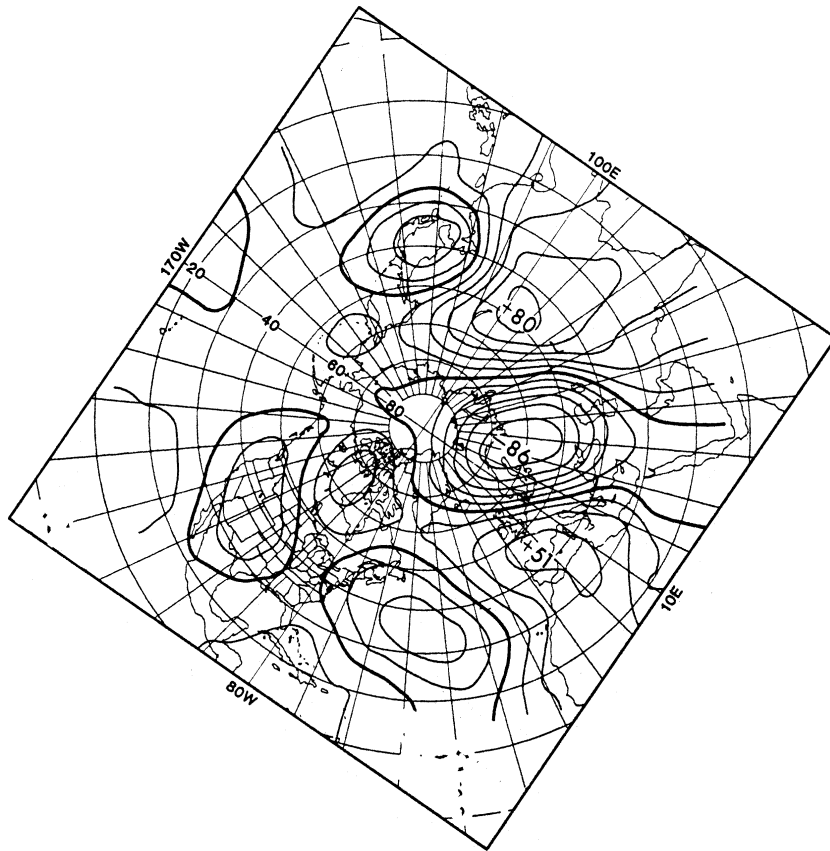


Figure 10. The Scandinavian pattern in November as depicted in the RPCA of Barnston and Livezey [4].

Figure 11 shows the daily time series of the Scandinavian pattern index from September 2000 until January 2001. The persistent, strongly positive phase of the pattern observed from mid September until early December may have been partially responsible for the anomalous circulation which prevailed over Europe resulting in the wettest autumn in England and Wales since records began (1766) and in exceptionally high temperatures over Central and Northern Europe. This period was dominated by the presence of a blocking anticyclone in north-western Russia and unusually low geopotential height values over Great Britain.

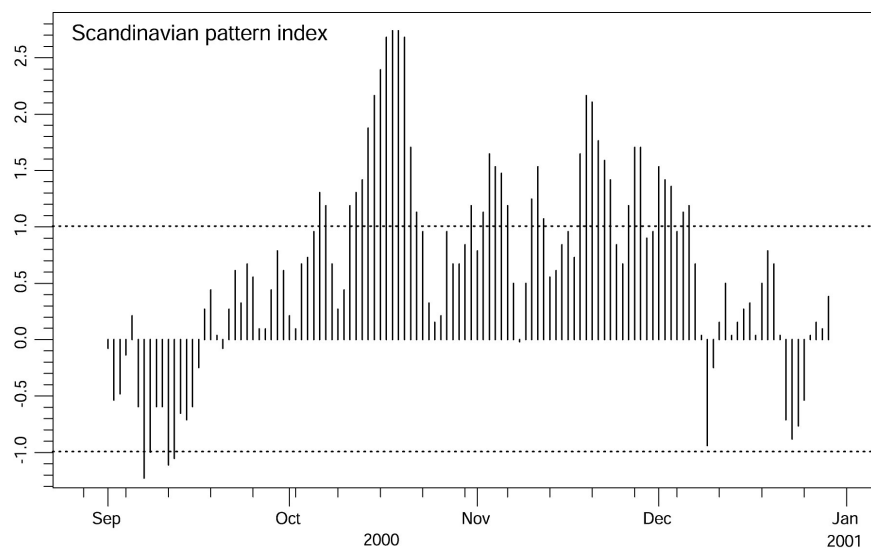


Figure 11. Daily amplitude (standardised PC) of the Scandinavian pattern from September 2000 to the end of December 2000 (data kindly supplied by Gerry Bell at the Climate Prediction Centre). Note the unusually long persistence of positive values that led to many flooding events in England and Wales. Dotted lines indicate one standard deviation above and below the long-term mean value of zero.

The structure of the Scandinavian pattern can be explained by the propagation of equivalent barotropic Rossby wave trains (Hoskins and Karoly, [11]). The wave trains of alternating positive and negative geopotential heights originate from a region of thermal subtropical forcing (i.e. positive SST anomalies). For very low-frequency forcing, the response is characterised by a train of Rossby waves oriented along a great circle route. As the frequency of the forcing is increased, the orientation of the patterns becomes much more zonal as in the case of the Scandinavian pattern.

3.5 Eastern Atlantic/Western Russian pattern

The Eastern Atlantic/Western Russian (EAWR) pattern is a less prominent pattern which has two major and one secondary centre (Fig. 3e and 12). The two negatively correlated major centres are located over the British Isles and the Caspian Sea, whereas a weaker centre with sign like that of the British centre occurs over north-eastern China. The positive phase of the pattern is associated with anomalously high geopotential height values over Western Europe and Eastern Siberia and lower than normal height values over the Caspian Sea resulting in a northerly flow over most of Europe. The EAWR pattern was first identified by Horel [9] and the intermonthly and interannual analysis by Esbensen [7] contained some elements of the EAWR pattern but it is completely absent in the analysis of Wallace and Gutzler [32].

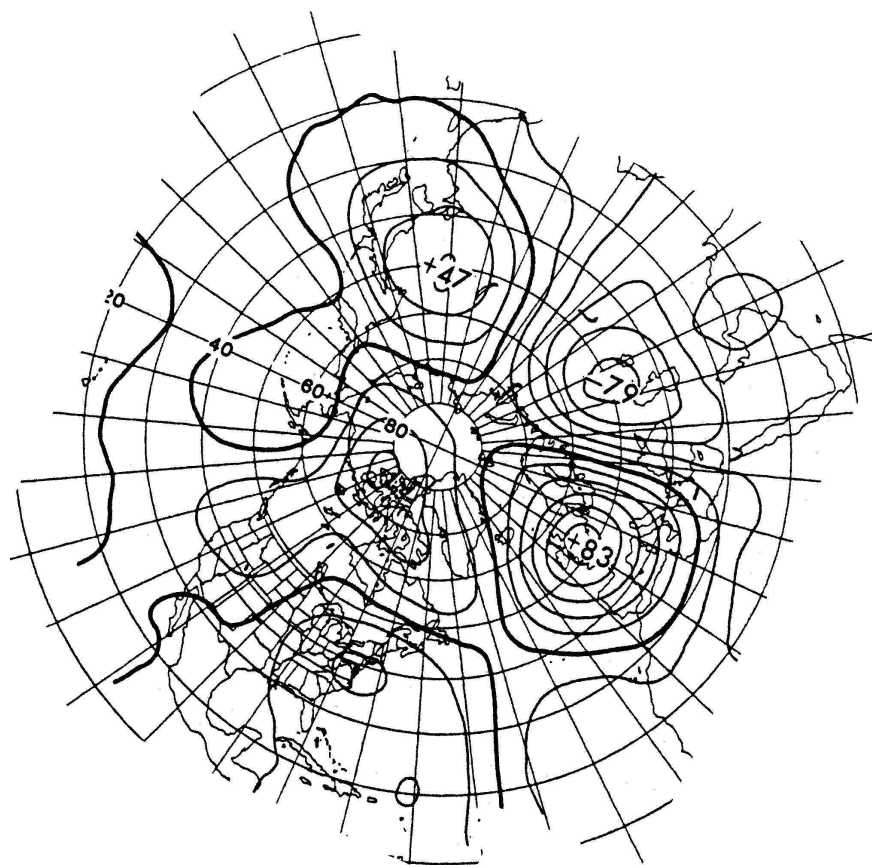


Figure 12. The Eastern Atlantic/Western Russian pattern in January as depicted in the RPCA of Barnston and Livezey [4].

The time series of the pattern (not shown) reveal considerable interseasonal and interannual variability. Persistent negative phases were observed during the winters and early springs of 1969/70, 1976/77 and 1978/79 characterised by enhanced precipitation in Western Europe and southerly flow over most of Europe. Pronounced positive phases of the pattern are less common.

3.6 Western Atlantic (WA) pattern

The Western Atlantic pattern (WA) is a rather ambiguous pattern, which is not reproduced by all the major teleconnections studies. Wallace and Gutzler [32] first identified it as a dipole shaped pattern in the western sector of the North Atlantic Ocean (Fig. 13) with negatively correlated centres in north-western Atlantic (55°N , 55°W) and near Bermuda (30°N , 55°W). They [32] noted that the two secondary regions of high correlation located over central Europe and northern China (40°N , 120°E) are associated with the Eurasian pattern. The positive phase of WA corresponds to a weak jet stream over the western Atlantic, a weak Icelandic low and a weak Azores high. Lau [15] found that the WA pattern is associated with changes in the intensity of the storm track over the eastern coast of North America, whereas Blackmon *et al.* [6] pointed out that WA flanks the North Atlantic jet stream.

There is a close resemblance between the WA and NAO, which raises doubts about the WA identity as a major teleconnection pattern. For example, patterns in the 1000-500 hPa thickness fields, associated with the WA, are very similar to those associated with the NAO. With regard to SLP, the WA exhibits the same pattern as the NAO with a shift in the position of its centres westward by approximately 20° of longitude. The WA pattern has been identified by Wallace and Gutzler [32] in their independent data set and also by Esbensen [7] in the intermonthly band. Esbensen, however, noted that the WA pattern is probably not independent as it exhibits correlations with several centres over Eurasia. Horel [9] found a similar pattern in the western sector of Northern Atlantic with two centres being shifted slightly to the north-west. The WA pattern was also identified by Blackmon *et al.* [6] and Kushnir and Wallace [14] with approximately the same structure and characteristics. Blackmon *et al.* [6] showed that WA pattern is stronger when interannual variability is removed, whereas Kushnir and Wallace noted that WA stands out better in the month-to-month variability.

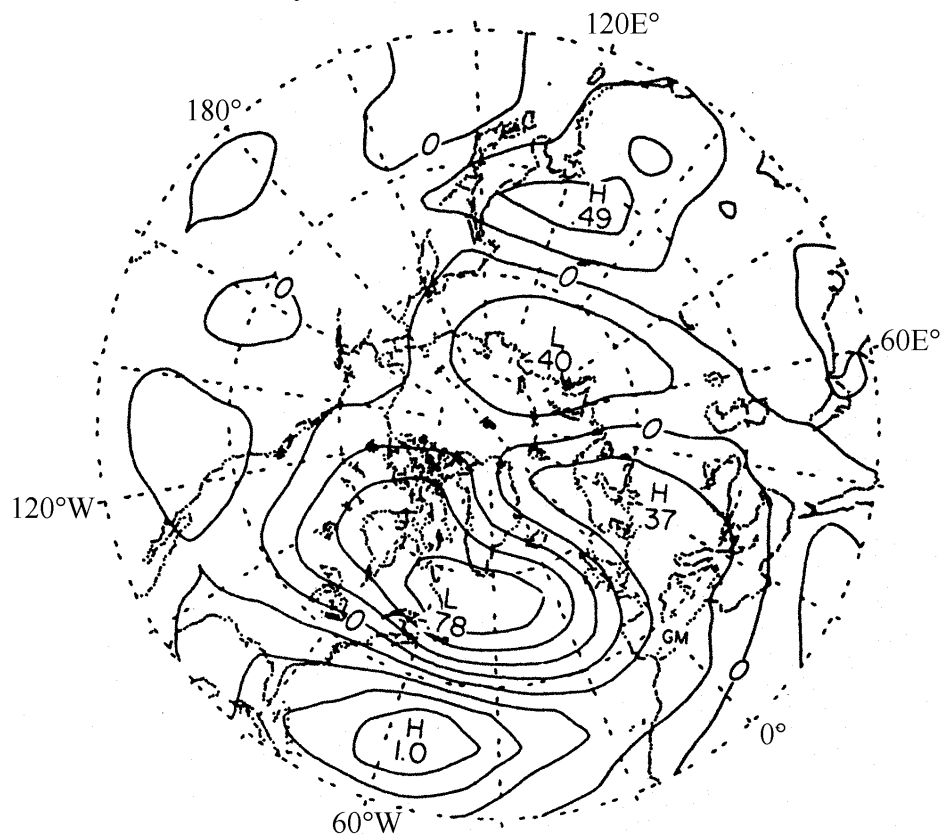


Figure 13. One-point correlation map showing correlation coefficients between SLP at the grid point 30°N , 55°W and SLP at every grid point (from Wallace and Gutzler, [32]).

It is the lack of independence, its similarity to the NAO and the fact that WA has not been identified in some of the major teleconnection studies (e.g. Barnston and Livezey, [4]) that make WA a rather ambiguous pattern.

4. PACIFIC-NORTH AMERICAN SECTOR TELECONNECTION PATTERNS

Five major teleconnection patterns have been found in the Pacific-North American sector with the PNA pattern being the most dominant and robust mode of low-frequency variability in that area.

4.1 Pacific/North American (PNA) pattern

The Pacific/North American pattern (PNA) is one of the most prominent modes of low-frequency variability in the NH mid-latitudes. It is comprised by four centres: one is located over the North Pacific Ocean (45°N , 165°W), a like-sign centre is found in south-eastern United States and the Gulf of Mexico and two centres of opposite sign are located in the southern sector of the North Pacific and central/western Canada (Fig. 3f and 14).

The positive phase of the PNA is associated with a deeper than normal Aleutian low, extensive ridging in north-western Canada and troughing in south-eastern United States resulting in a more wave-like 500 hPa geopotential height field with enhanced meridional flow. The negative phase of PNA is indicative of anomalies in the opposite sense with a more zonally oriented 500 hPa height field.

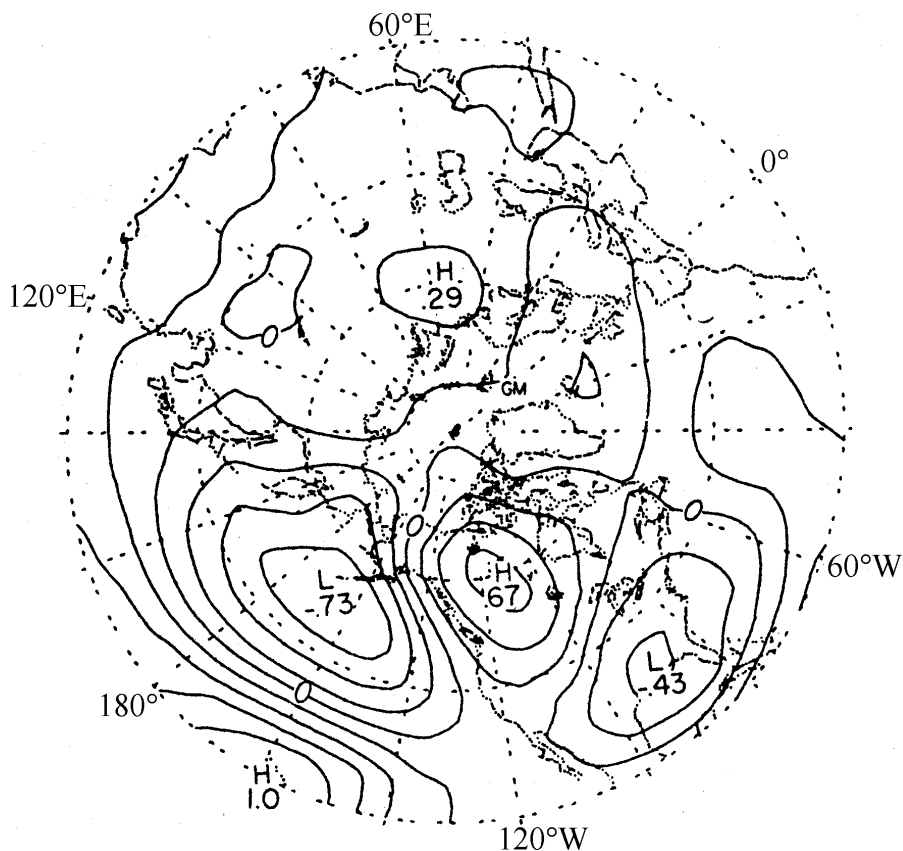


Figure 14. One-point correlation map showing correlation coefficients between SLP at the grid point 20°N , 160°W and SLP at every grid point (from Wallace and Gutzler, [32]).

The quadruple structure and persistence of the PNA pattern are confirmed by all the major teleconnections studies including Wallace and Gutzler [32], Barnston and Livezey [4], Esbensen [7] and Blackmon *et al.* [6]. The time series of the PNA index (not shown) suggests significant intraseasonal, interannual and interdecadal variability. A negative phase of the pattern dominated between 1964 and 1969, whereas the positive phase occurred from 1976 through to 1988. Of particular interest are the winters of 1976-1978 that were characterised by a persistent long-wave ridge along the western coast of North America (Namias, [17]).

It is a well-known fact amongst the weather forecasters in the United States that the PNA pattern has major implications for weather in North America. Lau [15] studied variability in the observed mid-latitude storm tracks in relation to low-frequency changes in the circulation patterns and concluded that north-to-south displacements of the storm track axis over eastern Pacific Ocean were linked to variability in the PNA pattern. For example, the low PNA index winter of 1957-1958 was characterised by a southward displacement of the Pacific jet stream, anomalously low 700 hPa heights over Alaska and above-normal heights over Hawaii (O'Connor, [18]). Horel and Wallace [10] suggested a possible relationship between PNA and the Southern Oscillation (SO). Their study of planetary-scale atmospheric phenomena associated with the SO showed how the positive phase of the PNA can be initiated by above normal SSTs in the central equatorial Pacific (Fig. 15). There are positive mid-tropospheric geopotential height anomalies over Canada and southern North Pacific and negative anomalies in the northern sector of North Pacific and south-eastern United States.

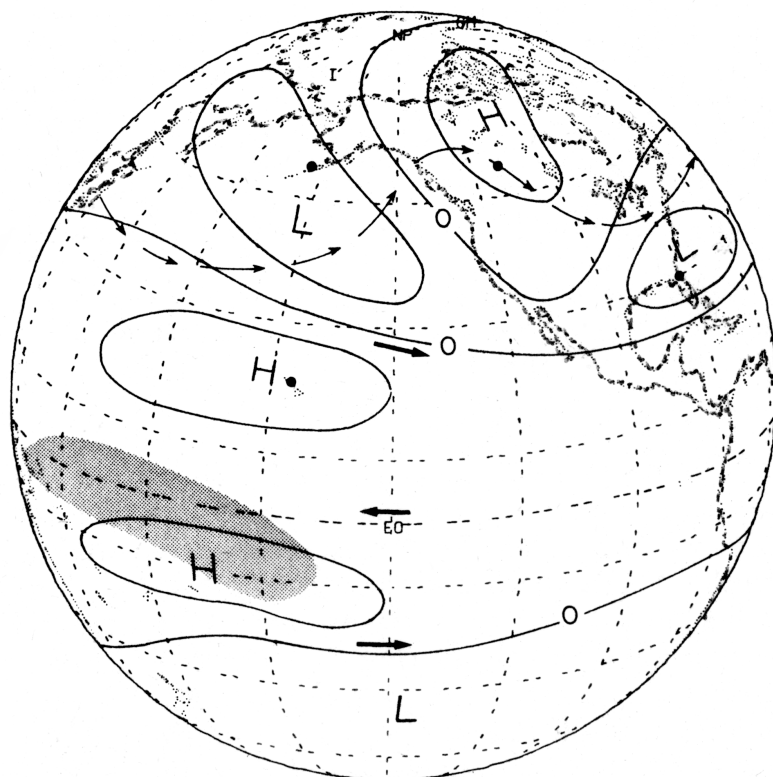


Figure 15. Schematic illustration of the global pattern of mid-tropospheric (700 hPa) and upper-tropospheric (300 hPa) geopotential height anomalies (solid lines) during a NH winter which coincided with an episode of warm SSTs in the equatorial Pacific. The arrows in bold show the strengthening of the subtropical jets in both hemispheres during warm episodes. The arrows in lighter type depict a mid-tropospheric streamline as distorted by the anomaly pattern, with pronounced ‘troughing’ over the central Pacific and ‘ridging’ over western Canada. Shading indicates regions of enhanced cirriform cloudiness and rainfall (from Horel and Wallace, [10]).

The distribution of geopotential height anomalies is consistent with modelling solutions (Hoskins and Karoly [11] and Webster [34]). Hoskins and Karoly [11] showed that wave trains (alternating positive and negative geopotential height anomalies spaced about 2000 km apart) develop in response to subtropical thermal forcing. The most prominent of these wave trains is oriented in such a way that the ray path connecting the anomaly centres is advected first poleward, then curves eastward and finally equatorward along a great circle route. The resemblance of their results with the PNA pattern shown in Fig. 15 is indeed striking.

4.2 Tropical/Northern Hemisphere pattern (TNH)

The Tropical /Northern Hemisphere (TNH) pattern was first identified by Mo and Livezey [16]. It consists of three centres (Fig. 3g): a major centre located just off the western coast of North America, another primary centre over the Hudson Bay which is negatively correlated to the first one and a weaker centre over Cuba and south-eastern Mexico. The positive phase of the TNH pattern is associated with a deeper than normal trough over the Hudson Bay and high values of geopotential height over western North America. Barnston *et al.* [3] showed that pronounced negative phases of the TNH pattern are often observed during El-Nino episodes. Barnston and Livezey [4] identified a similar pattern but with distinct differences in the location of the centres. The subtropical centre was shifted slightly north-east and two other centres were shifted westwards by at least 10°. The interannual signal of the zonally symmetric seesaw in Esbensen [7] clearly contains TNH with small differences.

4.3 Western Pacific (WP) pattern

The Western Pacific pattern (WP) is found in the western sector of North Pacific and is analogous to the WA pattern. It has a dipole structure with two strong, negatively correlated centres at 50°-60°N, 160°-180°E and 30°N, 160°-170°E (Fig. 3h and 16).

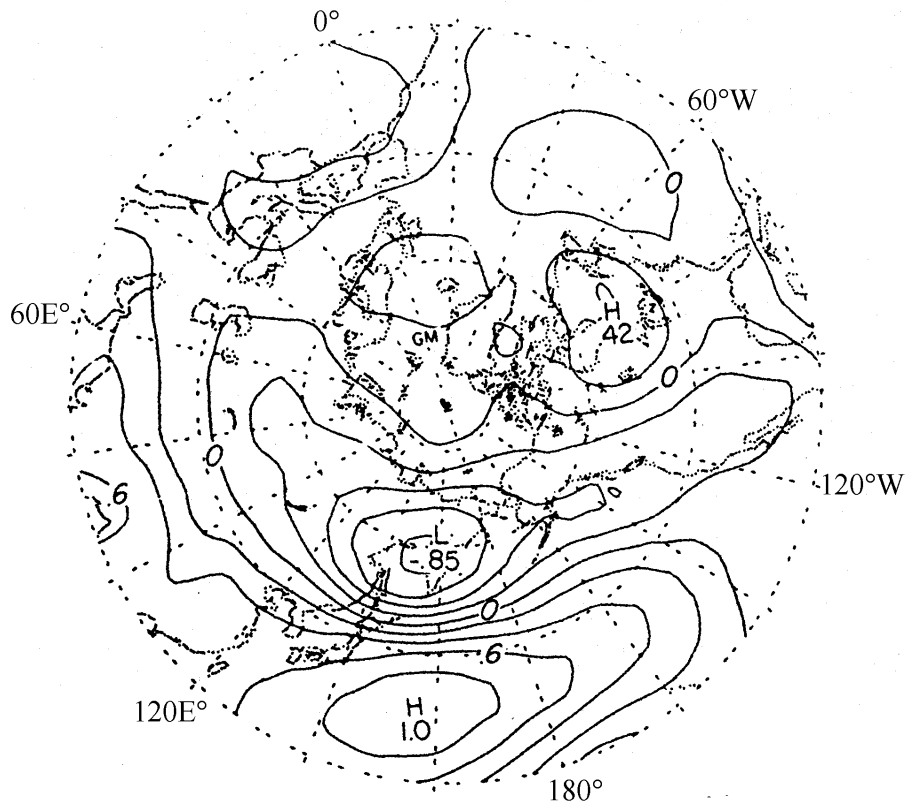


Figure 16. One-point correlation map showing correlation coefficients between SLP at the grid point 30°N, 155°E and SLP at every grid point (from Wallace and Gutzler, [32]).

The WP pattern is related to marked changes in the intensity of the entrance region of the Pacific jet stream and the associated storm track (Lau, [15]). Positive values of the WP index (not shown) are characterised by a weak Aleutian low and a weak jet stream over Japan. Wallace and Gutzler [32] noted that the SLP correlation fields of WP bear a strong resemblance to the North Pacific Oscillation (NPO) identified by Walker and Bliss [30]. They also showed that the WP pattern has an equivalent barotropic structure. Despite the strong correlation between the two centres, this pattern was not reproduced in Wallace and Gutzler's independent data set. It was confirmed, however, by all other major teleconnections studies with very small variations in structure and intensity. The WP pattern appeared clearly in Esbensen's [7] intermonthly band but not in the interannual one. Esbensen [7] noted that this

pattern explains a large proportion of the intermonthly variability in the western sector of the North Pacific and that it is essentially independent in space from variations in other regions of the Northern Hemisphere. WP was also confirmed by Barnston and Livezey [4] as what they referred to as the West Pacific Oscillation (WPO). The two centres were shifted slightly to the east compared with Fig. 16 and a weaker centre of like sign with the northern centre was identified in the southern and central United States (not shown). Blackmon *et al.* [6] showed that the WP loses its dipole structure on intermediate time scales (10-30 day periods) consisting rather of wave trains oriented from north-west to south-east. The WP pattern exhibits considerable intermonthly and interannual variability and it is also characterised by persistent high or low index episodes.

4.4 Eastern Pacific (EP) pattern

The Eastern Pacific pattern (EP) is one of the least prominent teleconnection patterns. It involves a north-south dipole of geopotential height anomalies over the eastern North Pacific. The northern centre is located over Alaska, with an opposite signed centre near Hawaii (Fig. 3i and 17). The positive phase of the EP pattern is associated with lower than normal geopotential height values over Alaska and western North America and higher than average values of geopotential height further south. This pattern results in an enhanced westerly flow over western North America with a north-eastward displacement of the Pacific jet stream. The negative phase of the EP pattern is characterised by a weaker westerly flow over western North America and, occasionally, the existence of a blocking anticyclone further east.

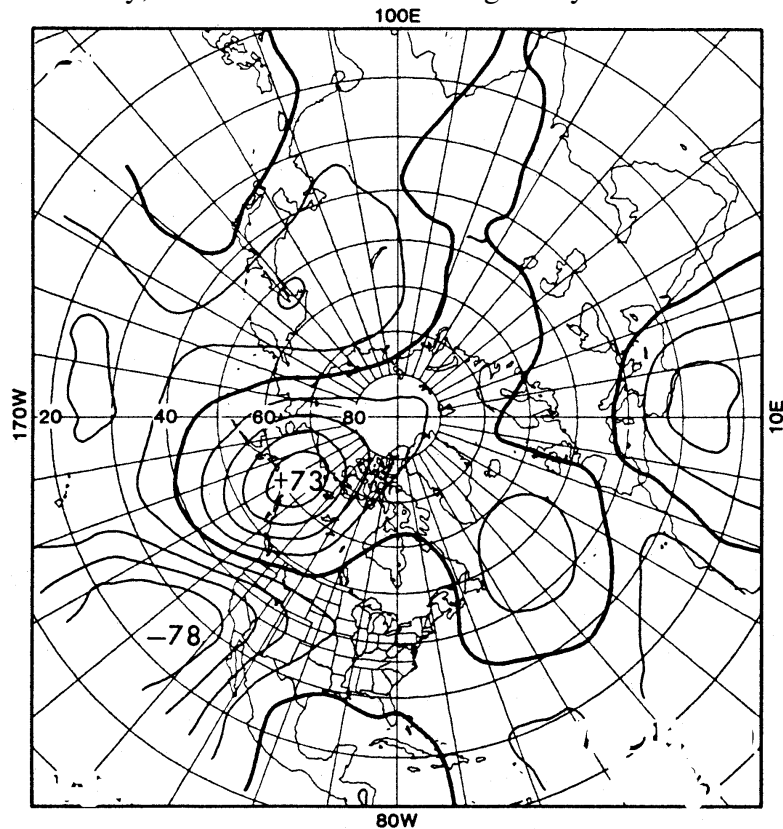


Figure 17. The Eastern Pacific (EP) pattern in January as depicted in the RPCA of Barnston and Livezey [4]).

The EP pattern was first identified by Horel [9], and named by Barnston and Livezey [4] (Fig. 12), who noted though that it was the weakest mode of their RPCA. Esbensen [7] found a similar pattern in the interannual band of his study (he referred to as the North Pacific pattern) but the dipole structure was less evident.

The EP index exhibits strong interannual and interdecadal variability (not shown). The index was predominantly negative from 1960-1973, then a sharp and persistent reversal occurred in the period 1973-1975 with a return to persistent negative values during the last 10 years. The strong, persistent negative

index episode of the period 1992-1993 was characterised by a stronger than normal subtropical jet stream which was displaced towards the south-western United States. These conditions resulted in unusually strong precipitation in that region bringing an end to a prolonged drought (Bell and Basist, [5]).

4.5 North Pacific (NP) pattern

The North Pacific pattern is not confirmed by all major studies. It was first identified by Walker and Bliss [30] who found evidence of an analogue to the NAO in the Pacific sector. They referred to it as the North Pacific Oscillation (NPO) and related it to a north-south seesaw in SLP in the Pacific Ocean. They also described a related thermal pattern analogous to the NAO. The positive phase of the NPO is associated with a belt of lower than normal pressure extending from Eastern Siberia through Canada and an abnormally intense subtropical Pacific anticyclone. Associated with these pressure anomalies are higher than normal temperatures in Canada and south-eastern Asia and anomalously low temperatures in Eastern Siberia, the North Pacific and south-western United States. The evidence in favour of the NPO, presented by Walker and Bliss [30] was rather insufficient mostly because of the sparsity of available data and the marginal level of many correlations.

Rogers [22] undertook a more comprehensive study of the NPO by analysing a 72-year data set of monthly SLP, SAT and precipitation from the Northern Hemisphere. He defined the NPO in terms of negatively correlated temperatures between western Alaska-Eastern Siberia and western Canada. He confirmed most of the results obtained by Walker and Bliss [30] and in particular that the NPO is associated with the strength of the westerlies over the Pacific and North America, which in turn result from longitudinal variations in the mean position of the Aleutian low. The positive phase of the NPO (his Aleutian below mode) is characterised by an eastward displacement of the Aleutian low towards the Gulf of Alaska, higher than normal temperatures in Canada and anomalously low temperatures in the north-western Pacific. Rogers [22] noted that the NPO is associated with regional but not hemispheric variations in basic climatic variables as is the case for the NAO.

The NP pattern was also identified by Esbensen [7] in the interannual analysis of his study. It has a dipole structure with two negatively correlated centres over Alaska and the central North Pacific. Barnston and Livezey [4] found that the NP pattern is active mainly during spring and autumn having one centre north of the Bering Strait and two opposite signed centres over Korea and central North Pacific. The differences in structure and the active period of the NP pattern make it a rather ambiguous pattern which requires more research.

5. CONCLUSIONS

There have been many studies of low-frequency atmospheric variability, which have produced a diverse and occasionally confusing set of teleconnection patterns, dynamical modes and oscillations. Some patterns (e.g. NAO, PNA) have been shown to have a profound impact on weather and climate, whereas there have been less support and fewer studies for other patterns (e.g. WA, NP). Teleconnection patterns identified in some studies were not found in other studies, some patterns have been given different names by different researchers, while the same names were often given to different patterns. The main reason for this confusion is the lack of a universally accepted definition and the plethora of different variables, methods and criteria used in search of teleconnections. An attempt to reconcile the differences has been made in this chapter by presenting and describing all major teleconnection patterns of the wintertime NH circulation.

Most teleconnections studies use statistical methods to identify and describe teleconnection patterns. Glantz [8] points out that the problems of autocorrelation (the effect of temporal correlation on the identification of leading relationships and the reliability of estimated cross correlations) and multiplicity (the subjective selection of only the largest correlation coefficients as relevant) have not been fully appreciated by the meteorological community. The study of teleconnection patterns will undoubtedly be a focus of major research interest in the future.

Acknowledgements

The authors wish to thank Dr Gerry Bell and Dr Mike Halpert at NCEP Climate Prediction Centre for their kind help in providing the RPCA time series and EOF data. David B. Stephenson would also like to thank the Bjerknes Centre for Climate Research for the opportunity to present this work at a workshop on 9-10 September 2002. The American Meteorological Society (AMS) is also acknowledged for kindly giving permission to use figures from its publications.

References

- [1] Ambaum, M.H.P., Hoskins, B.J., and Stephenson, D.B., *J. Climate* **14** (2001) 3495–3507.
- [2] Ångström, A., *Geografiska Annaler* **17** (1935) 242-258.
- [3] Barnston, A.G., Livezey, R.E., and Halpert, M.S., *J. Climate* **4** (1991) 203-217.
- [4] Barnston, A.G. and Livezey, R.E., *Mon. Wea. Rev.* **115** (1987) 1083-1126.
- [5] Bell, G.D. and Basist, A.N., *J. Climate*, **7**, (1994) 1581-1605.
- [6] Blackmon, M.L., Lee, Y.H., and Wallace, J.M., *J. Atmos. Sci.* **41** (1984) 969-979.
- [7] Esbensen, S.K., *Mon. Wea. Rev.* **112** (1984) 2016-2032.
- [8] Glantz, M.H., Katz, R.W., and Nicholls, N., 'Teleconnections linking worldwide climate anomalies' (Cambridge University Press, Cambridge, 1991) pp. 372.
- [9] Horel, J.D., *Mon. Wea. Rev.*, **109**, (1981) 2080-2092
- [10] Horel, J.D. and Wallace, J.M., *Mon. Wea. Rev* **109** (1981) 813-829.
- [11] Hoskins, B.J. and Karoly., D.J., *J. Atmos. Sci.* **38** (1981) 1179-1196.
- [12] Hurrell, J.W., *Science* **269** (1995) 676-679.
- [13] Jones, P.E., Jonnson, T., and Wheeler D., *Int. J. Climatol.* **17** (1997) 1433-1550.
- [14] Kushnir, Y. and Wallace, J.M., *J. Atmos. Sci.* **46** (1989) 3122-3142.
- [15] Lau, N.C., *J. Atmos. Sci.* **45** (1988) 2718-2743.
- [16] Mo, K.C. and Livezey, R.E., *Mon. Wea. Rev.* **114** (1983) 2488-2515.
- [17] Namias, J., *Mon. Wea. Rev.* **106** (1978) 279-295.
- [18] O'Connor, J.F., *Mon. Wea. Rev.* **86** (1958) 11-18.
- [19] Pavan, V., Molteni, F. and Brankovic, C., *Q. J. R. Meteorol. Soc.* **126** (2000) 2143-2173.
- [20] Pavan, V., Tibaldi, S., and Brankovic, C., *Q. J. R. Meteorol. Soc.* **126** (2000) 2125-2142.
- [21] Richman, M.B., *J. Climatol.* **6** (1986) 293-335.
- [22] Rogers, J.C., *J. Climatol.* **1** (1981) 39-57.
- [23] Schubert, S.D., *J. Atmos. Sci.* **43** (1986) 1210-1237.
- [24] Stephenson, D.B., Pavan, V., and Bojariu, R., *Int. J. Climatol.* **20** (2000) 1-18.
- [25] Stephenson, D.B., Wanner, H., Brønnimann, S. and Luterbacher J., The history of scientific research on the North Atlantic Oscillation. In: The North Atlantic Oscillation, Hurrell, J.W., Kushnir, Y., Ottersen G. and Visbeck, M. (Eds.), AGU, *in press*.
- [26] Thompson, D.W.J. and Wallace, J.M., *Geophys. Res. Let.* **25** (1998) 1297-1300.
- [27] Thompson, D.W.J. and Wallace, J.M., *J. Climate* **13** (2000) 1000-1016.
- [28] Thompson, D.W.J. and Wallace, J.M., *J. Climate* **13** (2000) 1018-1036.
- [29] van Loon, H. and Rogers, J.C., *Mon. Wea. Rev.* **106**, (1978) 296-310.
- [30] Walker, G.T. and Bliss, E.W., *V. Mem. Roy. Meteor. Soc.*, **4**, (1932) 53-84.
- [31] Wallace, J.M., *Q. J. R. Meteorol. Soc.* **126** (2000) 791-805.
- [32] Wallace, J.M. and Gutzler, D.S., *Mon. Weather. Rev.* **109** (1981) 784-812.
- [33] Wanner H., Brønnimann, S., Casty, C., Gyalistras, D., Luterbacher, J., Schmutz, C., Stephenson, D.B. and Xoplaki, E., *Survey Geophysics* **22** (2001) 321-381.
- [34] Webster, P.J., *J. Atmos. Sci.* **38** (1980) 554-571.